J|A|C|S COMMUNICATIONS

Published on Web 08/14/2009

Characterization of Iron−Carbonyl-Protected Gold Clusters

Olga Lopez-Acevedo,[†] Jyri Rintala,[‡] Suvi Virtanen,[‡] Cristina Femoni,[§] Cristina Tiozzo,[§] Henrik Grönbeck,[||] Mika Pettersson,[‡] and Hannu Häkkinen*[,†,‡]

Departments of Physics, Chemistry, Nanoscience Center, University of Jyväskylä, FI-40014 Jyväskylä, Finland, Dipartimento di Chimica Fisica ed Inorganica, Universita di Bologna, 40136 Bologna, Italy, and Department of Applied Physics and Competence Center for Catalysis, Chalmers University of Technology, SE-41296 Göteborg, Sweden

Received June 24, 2009; E-mail: Hannu.J.Hakkinen@jyu.fi

Ligand-stabilized nanometer-sized gold particles are interesting building blocks for molecular electronics, precursors for catalysts, optical labels for biomolecules and diagnosis, and potential nontoxic carriers for therapeutics.[1−3] All-gold-containing particles have traditionally been synthesized via reduction of gold salts in the presence of phosphines[2] or thiolates (SR).[3] Definite structural information is now available on thiolate-monolayer-protected Au clusters (SR-MPCs) thanks to X-ray structure determination of $Au_{102}(SR)_{44}$ and $Au_{25}(SR)_{18}$ clusters.[4] Theoretical efforts[5,6] have advanced hand-in-hand with experiments, which has yielded a clarified picture on how the surface-covalent gold-thiolate bond affects the stability of SR-MPCs. On the other hand, bimetal particles containing gold and near-end transition metals (Ni, Pd, Pt) in the core have been obtained from carbonyl chemistry, and many of them are structurally fully resolved.[7] In these particles, the Au/(Ni,Pd,Pt) ratio is well below unity, gold forms the inner part of the metal core, and the protecting carbonyl layer is bonded to the transition metal atoms. Most recently, some of us reported[8] a new organometallic approach to synthesize carbonyl-protected Au−Fe particles by reducing gold salts with $Fe_3(CO)_{11}^{2-}$. Five new species were isolated and structurally resolved, namely (**1**) $\{Au_5[Fe(CO)_4]_4\}^{3-}$, (**2**) $\{Au_{21}[Fe(CO)_4]_{10}\}^{5-}$, (**3**) $\{Au_{22}[Fe(CO)_4]_{12}\}^{6-}$, (**4**) $\{Au_{28}[Fe(CO)_3]_4[Fe(CO)_4]_{10}\}^{8-}$, and (**5**) $\{Au_{34}[Fe(CO)_3]_6[Fe(CO)_4]_8\}^{8-}$. The formal charges were attributed on the basis of the number of counterions per cluster in the crystal unit cell. The composition and structure of **1**−**5** differ dramatically from the known Au/(Ni,Pd,Pt) particles:[7] (i) the Au/Fe ratio exceeds unity and (ii) distinct Au_xFe_y structural units could be identified,[8] reminiscent of the predicted $(AuSR)_4$ rings and observed RSAuSR or $RS(AuSR)_2$ units in SR-MPCs. Here we report near-infrared (NIR) and Raman spectra of a truly monodispersed sample of **3**, interpret the NIR transitions from linear-response time-dependent density functional theory (LR-TDDFT), and show that bonding and electronic structure in these newly found compounds bear analogies to SR-MPCs. In particular, the frontier orbitals responsible for the NIR absorption of **2** and **3** are characterized in the framework of the "gold superatom model"[5a] which has successfully described the degree of metallicity and the surface-covalent bond in SR-MPCs.

A sample of **3** was prepared by reacting $[AuCl_4][NEt_4]$ with $[Fe_3(CO)_{11}][NEt_4]_2$ in a 1:1 molar ratio, according to literature and using standard Schlenk technique.[8] Its purity was confirmed by X-ray analyses performed on some of the crystals obtained by precipitation of its acetone solution with *n*-hexane. Furthermore, an IR spectrum of the acetonitrile solution was registered in a CaF_2 cell, showing a strong carbonyl absorption at 1990 cm^{-1} and a broad, weaker signal at ∼1920 cm^{-1}. The rest of the solid sample was dissolved in acetonitrile for absorption spectroscopy.

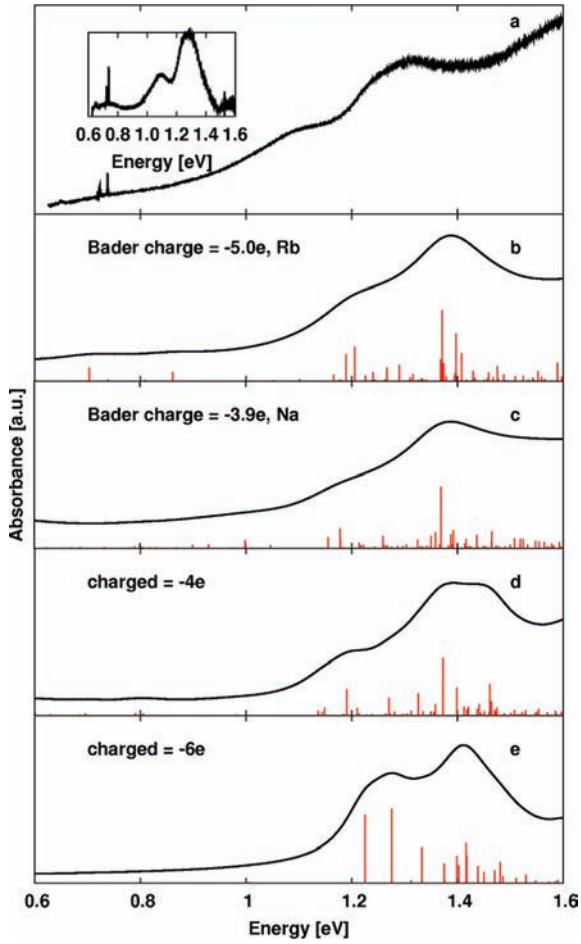

Figure 1. (a) NIR absorption spectrum of **3**, taken in acetonitrile. The inset shows the baseline-corrected spectrum which reveals a weak feature around 0.7 eV. (b−c) LR-(LB94)-TDDFT oscillator strengths of the model complex $Au_{22}[Fe(CO)_4]_{12}X_6$ built from the crystal structure of **3** (ref 8) with counterions Rb in (b) and Na in (c). The counterions yield a partial charge transfer to the gold−iron−carbonyl complex, and the calculated Bader charges of the complex are indicated in the panels. (d−e) Same as (b) and (c), without the counterions but with formal charges indicated in the panels. The theoretical oscillator strengths are folded by 0.05 eV Lorentzians. LR-(PBE)-TDDFT calculations for the PBE-relaxed **3** give a similar response with slight red shifts (by ∼0.1 eV) of the two absorption bands.

The NIR spectrum in the region 4500−13 000 cm^{-1} (0.56−1.61 eV) was measured with a Nicolet Magna 760 spectrometer by using a Quartz beamsplitter, an MCT detector, and a glass cuvette with a 5 mm optical path. Pure solvent was used as background, and 500 scans were averaged with a resolution of 2 cm^{-1}. The results

[†] Department of Physics, University of Jyväskylä.
[‡] Department of Chemistry, University of Jyväskylä.
[§] Universita di Bologna.
[||] Chalmers University of Technology.

10.1021/ja905182g CCC: $40.75

are shown in Figure 1a. Two strong absorptions are seen at 10 300 cm^{-1} (1.28 eV) and 8800 cm^{-1} (1.09 eV), and a weak absorption at 5800 cm^{-1} (0.72 eV) can be observed clearly in the baseline corrected spectrum (see inset). The sharp features at ~6000 cm^{-1} (0.74 eV) are produced by the strong combination/overtone absorptions of the solvent. The mid-IR spectrum of the compound was also measured in a CaF_2 cuvette, confirming the identity of the studied species. The gold cluster was observed to decompose under prolonged exposure to ambient air, after which the absorptions completely disappeared.

Further characterization of the compound in the powder form was made by micro-Raman spectroscopy, and the results are presented in Figure S1. The most characteristic feature in the spectrum is a broad band centered at 250 cm^{-1} which can be taken as a fingerprint of the compound. In addition, other weaker bands are observed at 418 and 663 cm^{-1}. A band at 250 cm^{-1} may be due to Au−Au or Au−Fe vibrations, but more detailed vibrational analysis is out of the scope of this report.

The electronic structure and NIR response of cluster compounds **1**−**5** were investigated using the GPAW code.[9] The exchange-correlation (xc) interaction was approximated by using either a Perdew−Burke−Ernzerhof (PBE)[10a] or van Leeuwen−Baerends (LB94)[10b] functional. NIR absorption (up to 1.6 eV) was calculated using the LR-TDDFT implementation in GPAW.[9b] The LB94 functional was used for generating the Kohn−Sham orbital basis and the xc part of the kernel in the LR-TDDFT calculations. Charge decomposition to cluster atoms was analyzed using the Bader method.[11] Further details are given in the Supporting Information (SI).

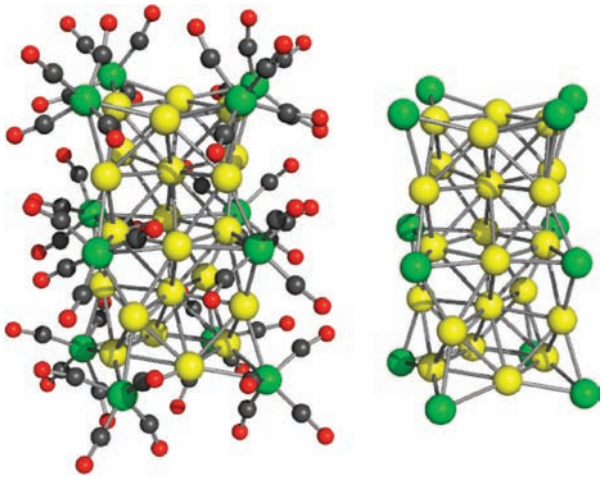

Figure 2. Left: Structure of cluster **3** from the experimental coordinates (ref 8). Right: the Au_{22}−Fe_{12} frame. Au, yellow; Fe, green; C, black; O, red.

The structure of **3** is shown in Figure 2. It can be described[8] as a five-layer stacked structure of alternating $Au_4[Fe(CO)_4]_4$ and Au_5 moieties with a slight twist between each $Au_4[Fe(CO)_4]_4$ moiety. The Au core is strongly prolate-deformed (cigar-like or rod-like), and Fe coordination to Au is 3-fold at the end layers and 4-fold in the middle layer.

In the experimental structure and with the assigned formal charges, **1**−**5** were found to have clear energy gaps (from the LB94 ground-state calculations) between the highest occupied molecular orbital (HOMO) and the lowest unoccupied one (LUMO); see Table S1 for details. Clusters **1** and **3** were further structurally relaxed using the PBE functional: **1** in its formal charge of −3 and **3** by relaxing a neutral model complex $Au_{22}[Fe(CO)_4]_{12}X_6$ where X = Rb, Na ions are used as model counterions instead of the NEt_4^+ ions used in the experiment. Relaxation does not change the underlying geometry but increases the mean interatomic distances by 2.8−3.5% for Au−Au, 1.5−2.3% for Au−Fe, and 2.3−5.3% for Fe−C (Table S1). This is a typical feature of the PBE functional.

In the LR-(LB94)-TDDFT calculations of the NIR response of **3**, we varied the effective charge of the cluster complex by varying the counterion (Rb yields a stronger charge-transfer than Na) or by charging the isolated cluster with 4 to 6 negative charges. The calculated oscillator strengths are shown in Figure 1b−e. All the considered cases yield spectra with consistent main features, which include a concentrated "band" of transitions around 1.25 and 1.4 eV. These compare favorably to the two measured bands at ~1.1 and ~1.3 eV (Figure 1a).

We analyze here first the absorption bands calculated for the $\{Au_{22}[Fe(CO)_4]_{12}\}^{6-}$ without counterions in the experimental structure (Figure 1e). The frontier orbital energy levels are shown in Figures 3 (left) and S2. These orbitals, delocalized over the Au_{22} core, are derived from Au(6s6p) atomic orbitals. Six orbitals are located in energy range −0.2 to 1.2 eV, with a degenerary pattern 1, 1, 3, 1 (where the LUMO is approximately 3-fold degenerate). Global angular momentum analysis (details in the SI) indicates that these states have major P, D, or mixed SD character (corresponding to angular momenta $L = 0-2$). Figure S3 shows that the first absorption band centered around 1.25 eV has transitions mainly from HOMO−1 to LUMO orbitals while the second band at around 1.4 eV has a more mixed character with contributing transitions HOMO−1 to LUMO+1, HOMO to LUMO+1 and from the Au(5d) band to LUMO.

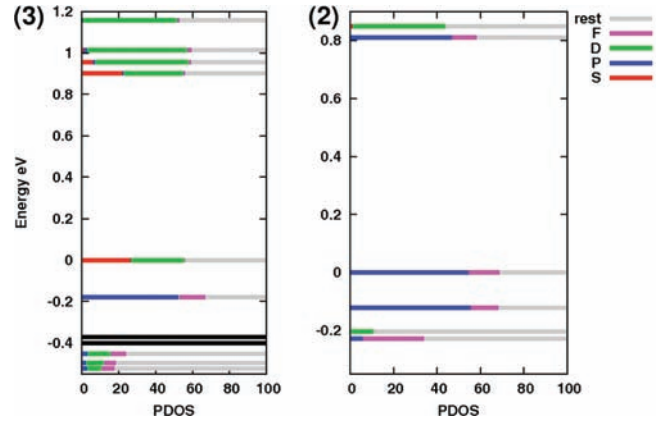

Figure 3. Kohn−Sham single particle states (LB94 functional) in the HOMO−LUMO regions of cluster **3** (left) and **2** (right). The colors denote weights of different L components in the spherical harmonics projection (PDOS) of the Kohn−Sham states in the gold core. Grey ("rest") denotes the summed weights of components higher than F symmetry (L > 3). Black states are combinations of Au(5d) and Fe(3d). The HOMO state is at zero energy.

We note that the weak and broad experimental feature at 0.7 eV (inset to Figure 1a) is absent from the theoretical absorption spectra calculated for **3** at the formal charge −6 (Figure 1e). Very weak transitions below 1 eV appear in the calculations when considering charges −4 to −5 (Figure 1b−d). In those cases, the HOMO of **3** is partially or completely depleted. These new transitions are mainly from Au(5d) to the depleted HOMO of the complex. This information suggests that the experimentally observed feature at 0.7 eV is owing to a true charge state of **3** in solution that is less than −6. This would then indicate weak cluster−counterion complexation, with possible impurity−water playing a role in association. This interpretation gets some support from the reported

dynamic light scattering result[8] which showed that the hydrodynamic diameter of the particles of **3** in solution is clearly larger than the mean diameter measured across carbonyl ligands of $\{Au_{22}[Fe(CO)_4]_{12}\}^{6-}$ in the solid state.

In this context it is interesting to note that the structure and shape of the slightly smaller compound $\{Au_{21}[Fe(CO)_4]_{10}\}^{5-}$ (**2**) was found to be very different from those of **3**.[8] In **2**, the Au core can be described as an Au-centered pentagonal antiprism Au_{11}, capped on both sides by pentagonal $Au_5[Fe(CO)_4]_5$ rings (Figure S2). Notable is the near-linear arrangement of Fe−Au−Fe bonds in this structure, similar to the RS−Au^I−SR bonds in protecting units of SR-MPCs.[4,5] The shape of the Au_{11} core is slightly oblate. The character of the frontier orbitals in the gold core (made out of the Au sp states) reflects the oblate shape, with the HOMO and HOMO−1 states displaying $P_{x,y}$ symmetry and LUMO the P_z symmetry (z parallel to C_5 axis); see Figures 3 (right) and S2.

These observed symmetries of the frontier orbitals in **2** and **3** can be rationalized by considering the bonding of $Fe(CO)_4$ units onto the gold core. Au−Fe interaction is strong; we find a binding energy of 3.97 eV for a single $Fe(CO)_4$ ligand in **1**. Interaction between Au(5d) and Fe(3d) bands yields a typical metal−ligand picture; see Figure S4 for the band analysis. Derived from the stable "18-electron" iron pentacarbonyl molecule, a single $Fe(CO)_4$ ligand can be considered as a two-electron acceptor (see Figure 4, which visualizes bonding of one $Fe(CO)_4$ onto **1**). Taking into account the number of Au atoms, $Fe(CO)_4$ ligands, and the formal charge, six and four sp ("free") electrons are left in complexes **2** and **3**, respectively, after applying counting rules in an analogous fashion to thiolate bonding to gold in SR-MPCs (where SR is a one-electron acceptor).[5a] Furthermore, this counting gives two free electrons for **5** and no free electrons for **1** and **4** ($[Fe(CO)]_3$ has to be considered as a four-electron acceptor in **4** and **5**).

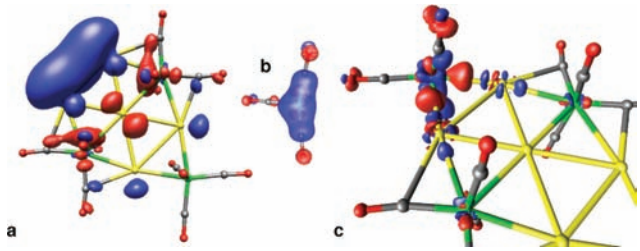

Figure 4. (a) HOMO of the incompletely protected cluster $Au_5[Fe(CO)_4]_3^{3-}$, showing the localization of the two "metallic" electrons in the Au−Au edge of the metal frame in a configuration reminiscent to σ bond of Au_2 dimer, (b) LUMO (acceptor level) of a single $Fe(CO)_4$ ligand, (c) difference in the electron density when cluster **1** is formed from the fragments shown in (a) and (b), visualizing the localization of the two "metallic" electrons in (a) to the Au−Fe bonds in **1**. Au, yellow; Fe, green; C, gray; O, red. In (a) and (b), red and blue denote different signs of the wave function, and in (c), they denote accumulation and depletion of charge, respectively.

In summary, we have reported a spectroscopic (NIR and Raman) and theoretical (absorption spectra and frontier orbitals) characterization of a new class of iron−carbonyl-protected gold clusters.[8] By drawing analogies to the well-known SR-MPC class of gold clusters, *we identified $Fe(CO)_3$ and $Fe(CO)_4$ units as the protecting ligands.* The NIR transitions detected for **3** can be explained in the framework of the "gold superatom model"[5a] which quantifies the "metallicity" of the gold core in terms of the effective number of itinerant electrons and accounts for the shapes and symmetries of the frontier orbitals contributing to transitions. These newly found compounds differ clearly from the earlier known carbonyl-protected bimetal Au/(Ni,Pd,Pt)[7] or pure transition metal[12] clusters and give a new dimension to the rich chemistry of gold-based "molecular metals".

Acknowledgment. We thank R. van Leeuwen and R. L. Whetten for discussions, the Academy of Finland and the Swedish Research Council for support, and the CSC (Espoo, Finland) for computer time.

Supporting Information Available: Details of theoretical methods and analysis, Table S1, and Figures S1−S4. This material is available free of charge via the Internet at http://pubs.acs.org.

References

(1) Whetten, R. L.; Khoury, J. T.; Alvarez, M. M.; Murthy, S.; Vezmar, I.; Wang, Z. L.; Stephens, P. W.; Cleveland, C. L.; Luedtke, W. D.; Landman, U. *Adv. Mater.* **1996**, *8*, 428. Templeton, A. C.; Wuelfing, M. P.; Murray, R. C. *Acc. Chem. Res.* **2000**, *33*, 27. Daniel, M.-C.; Astruc, D. *Chem. Rev.* **2004**, *104*, 293. Ackerson, C. J.; Jadzinsky, P. D.; Jensen, G. J.; Kornberg, R. D. *J. Am. Chem. Soc.* **2006**, *128*, 2635. Rosi, N. L.; Giljohann, D. A.; Thaxton, C. S.; Lytton-Jean, A. K. R.; Han, M. S.; Mirkin, C. A. *Science* **2006**, *312*, 1027. Albonetti, S.; Bonelli, R.; Mengou, J. E.; Femoni, C.; Tiozzo, C.; Zacchini, S.; Trifiro, F. *Catal. Today* **2008**, *137*, 483. Bowman, M.-C.; Ballard, T. E.; Ackerson, C. J.; Feldheim, D. L.; Margolis, D. M.; Melander, C. *J. Am. Chem. Soc.* **2008**, *130*, 6896. Tsunoyama, H.; Ichikuni, N.; Tsukuda, T. *Langmuir* **2008**, *24*, 11327.

(2) Schmid, G.; Boese, R.; Pfeil, R.; Bandermann, F.; Meyer, S.; Calis, G. H. M.; van der Velden, J. W. A. *Chem. Ber.* **1981**, *114*, 3634. Schmid, G. *Chem. Rev.* **1992**, *92*, 1709.

(3) Brust, M.; Walker, M.; Bethell, D.; Schiffrin, D. J.; Whyman, R. *J. Chem. Soc., Chem. Commun.* **1994**, 801. Chen, S.; Murray, R. W. *Langmuir* **1999**, *15*, 682. Schaaff, T. G.; Whetten, R. L. *J. Phys. Chem. B* **2000**, *104*, 2630. Quinn, B. M.; Liljeroth, P.; Ruiz, V.; Laaksonen, T.; Kontturi, K. *J. Am. Chem. Soc.* **2003**, *125*, 6644. Negishi, Y.; Nobusada, K.; Tsukuda, T. *J. Am. Chem. Soc.* **2005**, *127*, 5261.

(4) Jadzinsky, P. D.; Calero, G.; Ackerson, J. C.; Bushnell, D. A.; Kornberg, R. D. *Science* **2007**, *318*, 430. Heaven, M. W.; Dass, A.; White, P. S.; Holt, K. M.; Murray, R. W. *J. Am. Chem. Soc.* **2008**, *130*, 3754. Zhu, M.; Aikens, C. M.; Hollander, F. J.; Schatz, G. C.; Jin, R. *J. Am. Chem. Soc.* **2008**, *130*, 5883. Zhu, M.; Eckenhoff, W. T.; Pintauer, T.; Jin, R. *J. Phys. Chem. C* **2008**, *112*, 14221.

(5) (a) Walter, M.; Akola, J.; Lopez-Acevedo, O.; Jadzinsky, P. D.; Calero, G.; Ackerson, C. J.; Whetten, R. L.; Grönbeck, H.; Häkkinen, H. *Proc. Natl. Acad. Sci. U.S.A.* **2008**, *105*, 9157. (b) Akola, J.; Walter, M.; Whetten, R. L.; Häkkinen, H.; Grönbeck, H. *J. Am. Chem. Soc.* **2008**, *130*, 3756. (c) Lopez-Acevedo, O.; Akola, J.; Whetten, R. L.; Grönbeck, H.; Häkkinen, H. *J. Phys. Chem. C* **2009**, *113*, 5035. (d) Häkkinen, H.; Walter, M.; Grönbeck, H. *J. Phys. Chem. B* **2006**, *110*, 9927. (e) Häkkinen, H. *Chem. Soc. Rev.* **2008**, *37*, 1847.

(6) Li, Y.; Galli, G.; Gygi, F. *ACS Nano* **2008**, *2*, 1896. Gao, Y.; Shao, N.; Zeng, X. C. *ACS Nano* **2008**, *2*, 1497. Pei, Y.; Gao, Y.; Zeng, X. C. *J. Am. Chem. Soc.* **2008**, *130*, 7830. Jiang, D.; Tiago, M. L.; Luo, W.; Dai, S. *J. Am. Chem. Soc.* **2008**, *130*, 2777.

(7) (a) Whoolery, A.; Dahl, L. F. *J. Am. Chem. Soc.* **1991**, *113*, 6683. (b) Tran, N. T.; Kawano, M.; Powell, D. R.; Hayashi, R. K.; Campana, C. F.; Dahl, L. F. *J. Am. Chem. Soc.* **1999**, *121*, 5945. (c) Tran, N. T.; Powell, D. R.; Dahl, L. F. *Dalton Trans.* **2004**, 209. (d) Tran, N. T.; Powell, D. R.; Dahl, L. F. *Dalton Trans.* **2004**, 217. (e) Mednikov, E. G.; Tran, N. T.; Aschbrenner, N. L.; Dahl, L. F. *J. Cluster Sci.* **2007**, *18*, 253.

(8) Femoni, C.; Iapalucci, M. C.; Longoni, G.; Tiozzo, C.; Zacchini, S. *Angew. Chem., Int. Ed.* **2008**, *47*, 6666.

(9) (a) Mortensen, J. J.; Hansen, L. B.; Jacobsen, K. W. *Phys. Rev. B* **2005**, *71*, 035109. (b) Walter, M.; Häkkinen, H.; Lehtovaara, L.; Puska, M.; Enkovaara, J.; Rostgaard, C.; Mortensen, J. J. *J. Chem. Phys.* **2008**, *128*, 244101. GPAW is freely available at https://wiki.fysik.dtu.dk/gpaw.

(10) (a) Perdew, J. P.; Burke, K.; Ernzerhof, M. *Phys. Rev. Lett.* **1996**, *77*, 3865. (b) van Leeuwen, R.; Baerends, E. J. *Phys. Rev. A* **1994**, *49*, 2421.

(11) Henkelman, G.; Arnaldsson, A.; Jonsson, H. *Comput. Mater. Sci.* **2006**, *36*, 354. See also http://theory.cm.utexas.edu/henkelman/research/bader/.

(12) Femoni, C.; Iapalucci, M. C.; Kaswalder, F.; Longoni, G.; Zacchini, S. *Coord. Chem. Rev.* **2006**, *250*, 1580.

JA905182G